A 10-GHz High-Efficiency Lens Amplifier Array

Eric W. Bryerton, Manoja D. Weiss, and Zoya Popović

University of Colorado, Boulder, CO

Abstract— **The design of a 36-element quasi-optical amplifier for high-power and high-efficiency transmission at 10 GHz is presented. The following steps are taken in the design procedure: (1) design and characterization of a single high-efficiency CPW amplifier; (2) comparison to a saturated class-A amplifier; (3) design of a driver stage and testing of a two-stage CPW amplifier; (4) design of antennas and passive unit cell; (5) testing of active unit cell; (6) testing of passive lens array; and (7) construction and testing of active lens amplifier array. This systematic procedure enables us to ensure stability, calibrate properly, and measure power-combining efficiency as a function of the number of elements. A high-efficiency amplifier with 275 mW of output power, 48% power-added efficiency, and 6.4 dB saturated gain at 10.1 GHz gives 200 mW output power, 35% power-added efficiency, and 13 dB of saturated power gain in a two-stage amplifier. A single unit cell with second-resonant slot antennas gives the same performance and is the building block for a 36-element focal-point fed array.**

I. Introduction

Recently, there has been a great deal of interest in using quasi-optical power combining in the front end of medium-to-high-power transmitters. The advantages of this approach include:

- The output powers of many low-power devices can be combined in air eliminating feed lines with their associated loss and dispersion.
- The power-combining efficiency should remain constant as the number of elements increases. (One of the aims of this work is to verify this concept.)
- Several devices can fail with only slight dropoffs in the performance of the entire array. (This will also be tested in this work.)

Two limitations to this approach are feed efficiency and heat sinking. To improve feed efficiency, lens arrays similar in principle to Rotman lenses [1] have been developed. Here, the array is designed to be fed from a focal distance of 15 cm, reducing spill-over loss. Another problem with quasi-optical amplifier design for high power has been heat sinking. Solutions to this problem have included backing the array with liquid coolant [2]. This complicates the design of the antennas and adds considerably to the mass and complexity of the system. A more attractive solution is to eliminate the need for heat sinking by designing the amplifiers to have high efficiency. It was shown in [3] that a class-E amplifier can be integrated into a 5-GHz free-space, four-element power-combining array. Here, a class-E amplifier is used at 10 GHz to form a larger 36-element array with several Watts of output power and greater than 30% power-added efficiency.

II. Amplifier Design and Measurements

First, the final stage class-E amplifier is designed and measured. The class-E amplifier is a resonant switched-mode circuit in which a switch turns on at zero voltage and zero derivative of voltage. Ideally, the product of the switch voltage and current is zero, resulting in 100% efficiency. At microwave frequencies, however, an ideal switch is not available. A MESFET is driven as a switch and the matching circuitry is designed to approximate class-E operation at the fundamental and first harmonic. The device parasitic reactances are deembedded from the MESFET and included in the resonant circuit design.

The class-E amplifier here uses an Alpha AFM08P2 MESFET. The input match is designed for gain by measuring s_{11} in saturation. For class-E operation, the output circuit must present a fundamental impedance to the device of:

$$Z_{net} = \frac{0.28015}{\omega_s C_s} e^{j49.0524^\circ},$$

where $\frac{\omega_s}{2\pi}$ is the fundamental frequency, 10 GHz, and C_s is the transistor switch output capacitance, approximated by the small-signal C_{ds} of the MESFET, 0.21pF. The harmonics should all ideally be terminated in opens [4]. Using a single-stub transmission line match to satisfy the requirement of the fundamental impedance also presents a very high impedance to the second harmonic. It was shown in [3] that including only two harmonics in the design produces a good approximation of the required class-E waveforms at the output of the switch.

Coplanar waveguide (CPW) is chosen as the guiding structure to eliminate the need for vias from the source of the MESFET chips to ground. In order to be able to test the amplifier in a 50-Ω coaxial environment before integration into an array, a high-dielectric-constant, thick substrate is chosen, $\epsilon_r = 10.2$ and $h = 50\,\text{mil}$, to easily accomodate 50-Ω CPW transmission lines.

Using this class-E amplifier as the sole stage in an array would require an input power at the surface of the 36-element array of approximately 2.3 W. In order to more easily satisfy the input power requirements of the array, a driver stage is designed for high gain. The Alpha AFM04P2 MESFET is used for the driver stage. This device is similar to the device used for the class-E amplifier, but with half the gate periphery. Since this first stage could potentially provide more power than needed to sufficiently drive the second stage, it is desirable to operate the first stage at a class-C bias point, minimizing dissipated power while still maintaining sufficient gain. Fig. 1 shows the output power and power-added efficiency versus frequency for both the class-E second stage and the full two-stage amplifier.

To verify the effectiveness of the class-E approximation, a class-A amplifier is built and measured with the same MESFET, also at X-band. Fig. 2 compares the output power and power-added efficiency versus input power for the class-E and class-A amplifiers. Although the class-E design produces slightly less output power (295 mW) in saturation than the class-A (310 mW), the power-added efficiency of the class-E design is 46% as compared to 33% for the class-A.

III. Unit Cell

A second-resonant slot antenna is chosen as the radiating element for its easy integration with CPW transmission lines and low input impedance. A single antenna is built, measured, and compared to simulations using Hewlett Packard's MOMENTUM software. Fig. 3 shows the measured and simulated return loss for a single antenna. In order to conserve space in the array design, two of the four dc bias lines are routed through the side of the antenna opposite to the feed as shown in the schematic of the unit cell, Fig. 4. The RF is suppressed from these bias lines by 0.6 pF capacitors from the center conductor to ground. These capacitors and the bias lines are not included in the simulation. This accounts for the small frequency shift seen from simulation to measurement. The antenna has a measured 2:1 VSWR bandwidth of 7%. Measured E- and H-plane radiation patterns show the expected result that the antenna radiates 3-4 dB more into the dielectric. A polarizer can be placed a quarter wavelength from the backside to improve the directivity looking away from the dielectric. Cross-pol radiation is over 10dB below co-pol for the entire angular range.

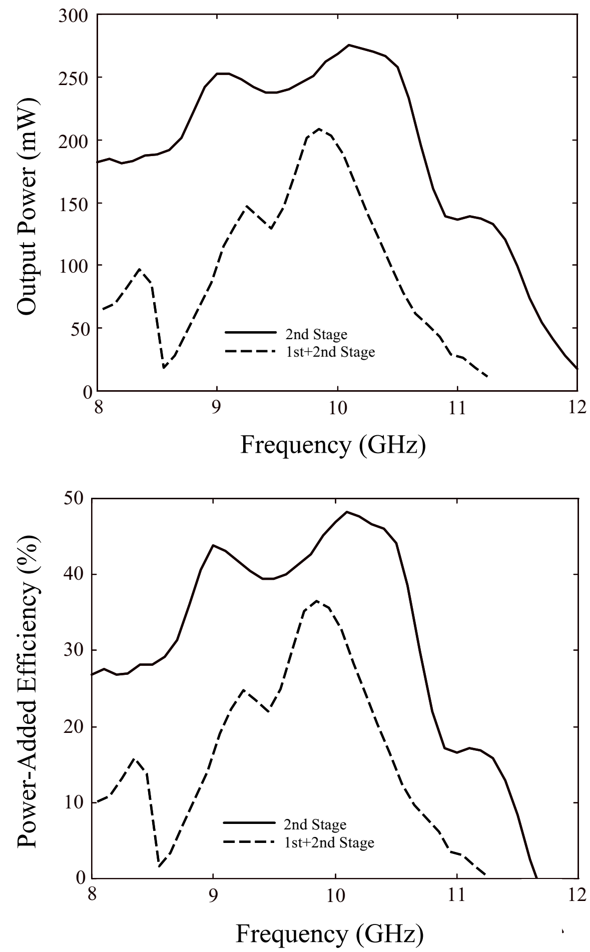

Fig. 1. Measured output power and power-added efficiency versus frequency for the class-E amplifier alone (solid line, P_{in}=18 dBm) and the class-E amplifier with a driver stage (dashed line, P_{in}=10 dBm).

This antenna is then connected to the input and output of the two-stage amplifier presented earlier. Fig. 4 shows the unit cell. A stabilization network consisting of a 0.6 pF capacitor in series with a 50-ohm resistor is placed from gate to source of the first stage since the amplifier is not unconditionally stable.

A passive unit cell is also fabricated with the amplifier replaced by a transmission line. This is used to calibrate the measurement of output power and efficiency of the active unit cell. Using this calibration, an output power of 214 mW is measured for the unit cell with a power-added efficiency of 36% and associated gain of 10.5 dB.

IV. Passive Array

A 36-element passive array is fabricated and is similar in appearance to the active array shown in Fig. 5, except the amplifier circuitry is replaced by a through

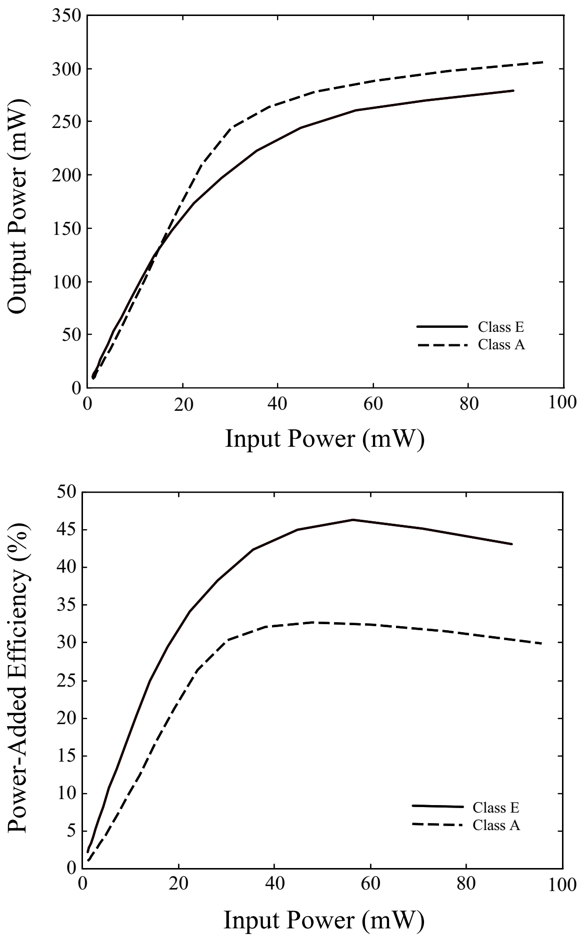

Fig. 2. Measured output power and power-added efficiency as a function of input power for the class-E amplifier alone (solid line) and the class-A amplifier (dashed line). Drain voltage, V_{DS}, is 4 V for the class-E and 5 V for the class-A. Drain current, I_{DS}, is 110 mA for the class-E and 140 mA for the class-A.

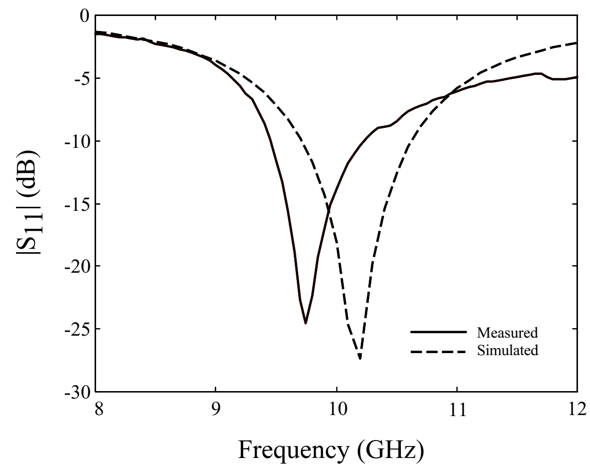

Fig. 3. Measured and simulated return loss for the center-fed second-resonant slot antenna. The slot is 9.8 mm long and 3.3 mm wide. The simulation does not include bias lines and capacitors.

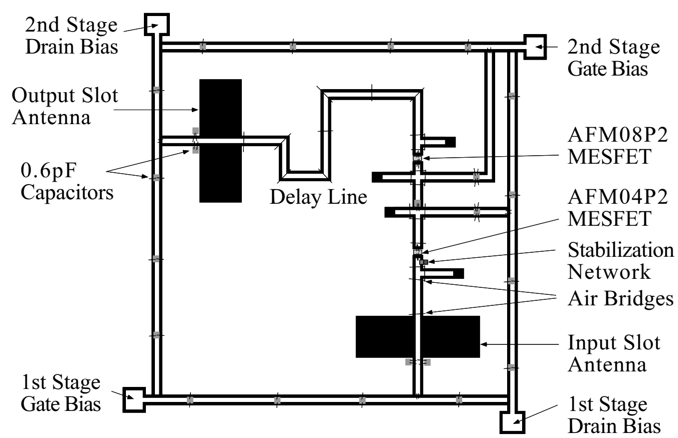

Fig. 4. Active unit cell which yields a transmitted power of 214 mW with 36% power-added efficiency at 10.1 GHz. The unit cell measures a free-space wavelength on each side, 3 cm.

line. As shown in the figure, the delay lines are longest in the center elements and shortest on the furthest corner elements. The relative lengths of the delay lines are calculated using the design equations for a lens with one degree of freedom [5]. The lens array is designed for a focal distance of $F = 15\,\mathrm{cm}$ corresponding to a $\frac{F}{D}$ ratio of 0.707. This gives a predicted spill-over loss of 2.2 dB.

The experimental setup used for making free-space measurements on the arrays and unit cells is shown in Fig. 6. For the 36-element array, the far field of the array is three meters. For the unit cell, R=15 cm. For calibration, the transmit and receive horns are co-polarized and the array is replaced by an aperture of the same size. Then the array is placed in the aperture and the transmit horn is rotated 90°. The gain of the array is measured relative to this through measurement. Fig. 7 shows this as a function of frequency. As indicated, a polarizer can be placed a quarter wavelength behind the array for added gain.

To see if the lens array is focuses, the received power is measured as a function of the feed distance, F. This is shown in Fig. 8. The measurement shows the focal point is actually at a distance of $F = 16.5\,\mathrm{cm}$. The ripple in this measurement is due to a standing wave formed between the transmit horn and the surface of the array indicated by the $\frac{\lambda}{2}$ periodicity of the ripple.

V. Active Array

A 36-element active lens array is fabricated and is shown in Fig. 5. The design of the delay lines is identi-

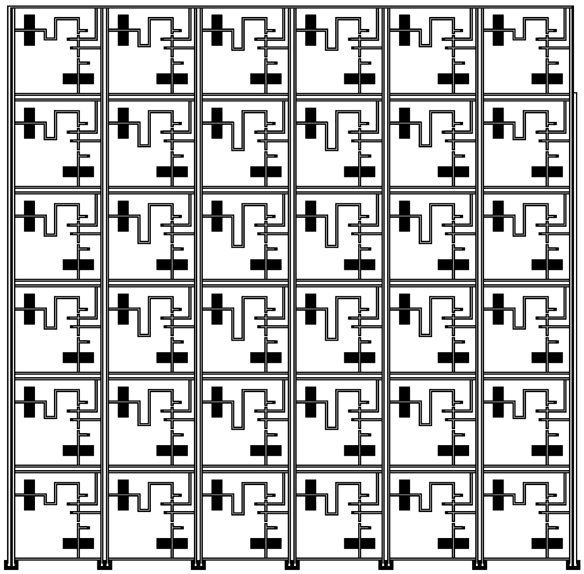

Fig. 5. Active 36-element array with delay lines designed to provide a focal distance for feeding of 15 cm.

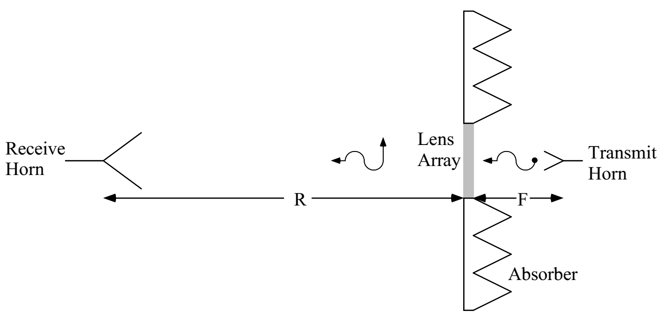

Fig. 6. Experimental setup for free-space unit cell and array measurements. F is the focal distance and R is in the far field of the array.

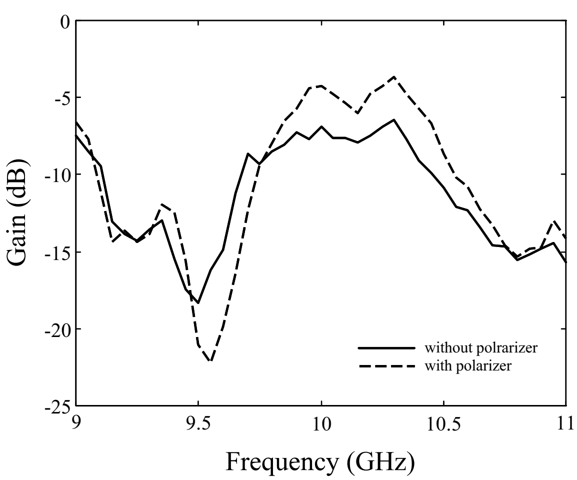

Fig. 7. Frequency sweep for passive 36-element array.

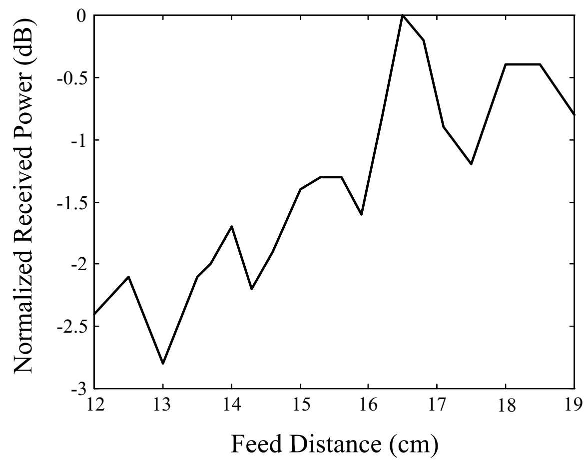

Fig. 8. Power received in far field versus feed distance. Maximum focusing occurs at a feed distance of 16.5 cm.

cal to the passive array. In a focal-point fed design, the elements across the array are not equally saturated. In this array, there is about 5 dB difference in input power levels between the center and corner elements. However, based on Fig. 2, we feel that this will not be a problem since both efficiency and output power remain relatively constant over a wide range of input power levels. This array is still being populated with devices. Measurements will be performed on a 2x2, 4x4, and 6x6 array to see if the power-combining efficiency remains constant as the number of elements increases. Based on power-combining efficiencies measured for similar arrays [3], [6], an output power of over 6 W is expected for the 36-element array.

VI. Acknowledgment

This work is supported by the University of Michigan under a MURI ARO program and Ansoft Corporation under an Air Force STTR Phase II.

References

[1] W. Rotman and R. Turner, "Wide angle microwave lens for line source applications," *IEEE Trans. Ant. and Prop.*, vol. 11, pp. 623–632, Nov. 1963.

[2] J. Hubert, J. Schoenberg, and Z. Popović, "High-power hybrid quasi-optical ka-band amplifier design," in *1995 IEEE MTT-S Int. Microwave Symp. Dig.*, (Orlando, FL), pp. 585–588, May 1995.

[3] T. B. Mader, *Quasi-Optical Class-E Power Amplifiers.* PhD thesis, Univ. of Colorado, Boulder, CO, 1995.

[4] T. B. Mader and Z. B. Popović, "The transmission line class-e amplifier," *IEEE Microwave and Guided Wave Lett.*, vol. 5, pp. 290–292, Sept. 1995.

[5] D. T. McGrath, "Planar three-dimensional constrained lenses," *IEEE Trans. Ant. and Prop.*, vol. 34, pp. 46–50, Jan. 1986.

[6] T. Berg, "High-gain quasi-optical lens amplifier array," Master's thesis, Univ. of Colorado, Boulder, CO, 1997.